Ocean Engineering 294 (2024) 116733

Contents lists available at ScienceDirect

Ocean Engineering

journal homepage: www.elsevier.com/locate/oceaneng

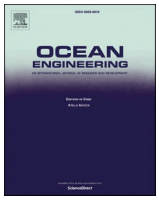

Research paper

Estimation of capacity decrease due to accumulated excess pore pressures around cyclically loaded offshore foundations in sand

Jann-Eike Saathoff *, Martin Achmus

Leibniz University Hannover, Germany

ARTICLE INFO

Keywords:
Contour plot
Cyclic element tests
Direct simple shear
Excess pore pressure accumulation
Finite element model
Foundation design
Monopile
Offshore
Partially drained conditions

ABSTRACT

In particular during storm events, a build-up of excess pore pressures may occur in the soil around cyclically loaded offshore foundations. Such accumulated excess pore pressure reduces the effective stresses in the soil and hence negatively affects the structural integrity. Even though the consideration of this degradation effect on the bearing capacity is commonly demanded by the involved certification or approval bodies, no generally applicable and accepted method for the calculative verification currently exists. The paper presents an approach which allows for the transfer of the soil behaviour observed in cyclic direct simple shear tests to the foundation structure system by means of a three-dimensional numerical model. The method is modular and can easily be assessed with engineering judgment in each substep. The used approach enables the consideration of site-specific cyclic laboratory test results by taking into account the mean stress, the cyclic shear stress amplitude and the number of load cycles at each integration point of the numerical model. Hence, the numerical approach may contribute to the optimisation of common foundation solutions as well as to the verification of innovative foundation structures even in complex soil conditions.

1. Introduction

In Europe, wind energy has taken a key role in the expansion of renewable energy supply in recent years. However, to reach the ambitious goals of the „European Green Deal“ plans of the European Union, a massive further expansion is necessary, which cannot be achieved without numerous new offshore wind farms. For instance, the German government plans an installed offshore wind power of 35 GW in 2035, which is more than four times the currently installed power.

In the offshore environment, the conditions for harvesting wind energy are favourable, but the additional wave loads acting on the support structures of wind turbine towers are challenging. Fig. 1 schematically shows frequently used support structures. In particular under storm conditions, numerous large loads induced by waves act on the foundation structure. Such cyclic loads can even in sand soils cause an accumulation of excess pore pressures in the soil around the foundation and with that a decrease in the ultimate capacity of the foundation. Although the consideration of cyclic degradation effects on bearing capacity due to excess pore pressures in the design is commonly demanded (e.g. DNV-RP-C212, 2019), no generally applicable and accepted method for the calculative verification currently exists. In fact, an estimation is possible with sophisticated numerical methods (cf. section 2). However, these methods are not suitable for practical design. Instead, in practice often simple criteria are considered. As an example, monopiles in sand soils under extreme load are often designed by considering „cyclic p-y curves“, which are believed to account for a capacity degradation of about 100 cycles of the considered extreme load (Dührkop, 2009; API, 2014). In a further check, it is proven that the effect of the design storm, consisting of numerous wave loads of different magnitudes, is not worse than these 100 cycles of the extreme load. The reliability of such highly idealized design approaches must be doubted. Therefore, there is a need for a simple and practically handable method to estimate accumulated excess pore pressures due to cyclic loads.

The paper at hand presents a new method for that purpose, which applies a relatively simple numerical simulation model and uses the results of undrained cyclic direct simple shear (DSS) tests as input data. The presented generic approach is intended to be used with any finite element software. The concept consists of a numerical reference calculation which is then combined with undrained cyclic laboratory test results (Achmus et al., 2018; Saathoff and Achmus, 2020). The concept is designed to account for the excess pore pressure accumulation and, thus, the capacity degradation due to cyclic lateral loading

* Corresponding author.
E-mail address: saathoff@igth.uni-hannover.de (J.-E. Saathoff).

https://doi.org/10.1016/j.oceaneng.2024.116733
Received 27 April 2023; Received in revised form 10 December 2023; Accepted 12 January 2024
Available online 27 January 2024

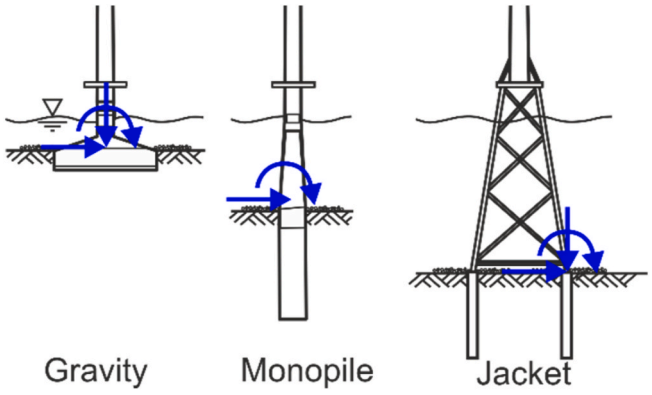

Fig. 1. Foundation structures (gravity based foundation, monopile and jacket foundation) for offshore wind energy turbines (schematic).

during a storm event in saturated, predominantly non-cohesive soils.

2. State of the art

To investigate the behaviour of soil elements under cyclic loading, various laboratory tests are carried out in practice (e.g. drained or undrained cyclic simple shear tests or cyclic triaxial tests). The soil behaviour determined in the element test needs to be transferred to the global soil-structure interaction problem by means of finite element simulations. For this purpose, different numerical approaches can be used, which can be classified into explicit and implicit procedures.

Implicit methods calculate the system behaviour cycle by cycle using a complex material law that describes cyclic soil behaviour as accurately as possible. The calibration can be very time-consuming, and the subsequent numerical calculation requires high computational effort. In addition, only a limited number of cycles can normally be dealt with, since unavoidable numerical errors accumulate and may become predominant after a large number of cycles. Suitable material laws are hypoplasticity with intergranular strain (Kolymbas, 1988; Von Wolffersdorff, 1996; Niemunis and Herle, 1998) and the simple anisotropic sand plasticity model (SANISAND) model (Dafalias and Manzari, 2004), for instance.

The hypoplasticity model with intergranular strain is an advanced material law describing sand behaviour both for monotonic and cyclic problems. Due to the intergranular strain extension by Niemunis and Herle (1998), it realistically describes the soil behaviour under repeated unloading and reloading, i.e. cyclic loading. The model does not distinguish between elastic and plastic parts as there is no plastic yield surface. The main advantage of hypoplasticity is that it is state-dependent and soil densification is approximated. In general, stress level, soil density, dilatancy, contractance and peak friction angle are considered with one single equation without a potential function for plastic or elastic deformation. The hypoplasticity model was frequently used in order to back-calculate small- or large-scale model tests. Taşan et al. (2010), Grabe et al. (2004) and Grabe et al. (2005) used a two-phase hypoplasticity model with intergranular strain for fully saturated soils to investigate the excess pore pressure within multiple cycles around monopiles and were able to identify several influencing parameters. Taşan (2011) identified influences of the number of cycles, the loading type, the relative density, the loading frequency, the soil permeability, and the pile diameter. Similar investigations were performed by Cuéllar (2011).

Other sophisticated implicit models are based on a critical state approach with an advanced dilatancy model and bounding surface plasticity. The simple anisotropic sand plasticity model (SANISAND) was derived based on the critical state two-surface model with an open wedge yield surface in the stress space for sands by Manzari and Dafalias (1997) and the bounding surface plasticity (Dafalias and Popov, 1975; Dafalias, 1986). The bounding surface envelopes the possible stress states and the dilatancy surface separates contractive from dilative behaviour. There is an additional yield surface for the current stress state. As a drawback, the original SANISAND model often overestimates the liquefaction potential and more recent versions, which are more accurate in this regard, still need a large number of input parameters for which the calibration can be tedious. There are also many other cyclic models in addition to the SANISAND constitutive laws, whereby all models have different advantages and disadvantages, as no implicit model can currently be considered universally applicable.

Besides the use of complex material models with up to 20 material parameters, explicit models are often used, in which the cyclic system response is based on the results of high-quality cyclic laboratory tests. Explicit methods calculate only individual load steps to capture the cyclic loading conditions of the system and then transfer the results of cyclic laboratory tests to the system. This means that any number of load cycles can be taken into account and the calculation effort is appreciably reduced compared to an implicit method. They can be used to estimate excess pore pressure accumulation with a very limited number of calibrated soil parameters. First explicit approaches with simple pore pressure generation and dissipation can be found in Rahman et al. (1977), Jostad et al. (1997) and Taiebat (1999).

An up-to-date explicit model is the High Cycle Accumulation (HCA) model. It bases on extensive laboratory work on drained cyclic triaxial and DSS tests (Wichtmann, 2005). Within the HCA, the first cycles are calculated implicitly and used for the explicit part of the model to use an empirical regression of laboratory results (Niemunis et al., 2005; Wichtmann, 2005). An implicit control calculation can be performed after a certain number of load cycles. Several element tests with up to 10^6 cycles are used for the empirical regression. The HCA is an explicit method which requires different sub-functions to consider the different influences found in cyclic soil tests. The intensity of the strain accumulation of a soil element is derived from the functional approach given in Equation (1).

$$\dot{\varepsilon}_{acc} = f_N \, f_\pi \, f_{ampl} \, f_p \, f_Y \tag{1}$$

The factors are functions which consider the load history (f_N), the polarization (f_π), the strain amplitude (f_{ampl}), the confining pressure (f_p) and the stress ratio (f_Y) and the void ratio as main state variable. The model was used intensively for validation and calibration with a large amount of laboratory tests. Good agreement was found in back-calculations of cyclic laboratory tests in Wichtmann et al. (2011). All parameters can be established with a limited number of cyclic triaxial tests. The method is theoretically very well founded, but is more suitable for basic scientific investigations and less for practical applications. The validation and various applications are presented in Zachert and Wichtmann (2020) and Jostad et al. (2020).

A method for predicting the load-bearing behaviour of foundation structures under cyclic loading that is conceptually applicable to a variety of general cyclic problems was presented by Jostad and Andresen (2009) and is based on ideas according to Andersen (1976) and Andersen et al. (1978). They combine the information from site-specific cyclic direct simple shear and cyclic undrained triaxial tests in the form of contour plots as input for the numerical simulations. The general approach is based on the stress path philosophy (Lambe, 1967; Bjerrum, 1973). Herein, representative tests are chosen for representative stress states of elements. It implies that different laboratory test results can be seen as representative and be used to describe the soil response (Wood, 1990). In general, this requires true triaxial tests; however, since these are not feasible for practical application, triaxial tests and direct simple shear tests are used. The main model assumption is that the element follows exactly the assumed stress path. By using the contour plots for different representative load types over the number of cycles, no separate constitutive framework is needed due to the additional inter- and extrapolation of laboratory results. Thereby, the undrained cyclic accumulation model (UDCAM) was mainly developed for the soil response of material with negligible drainage. Hence, no separate

dissipation analysis is considered in this model. The soil response of sandy material is more complex due to dilatancy and drainage effects. Therefore, the partially drained cyclic accumulation model (PDCAM) was developed (Andersen et al., 1994; Jostad et al., 1997). Based on the dissipated excess pore pressure, PDCAM also predicts the volumetric strain after the number of cycles. It can hence estimate the deformation after the storm – similar to the stiffness degradation method (SDM) by Achmus et al. (2009). The PDCAM model works in a similar way as the UDCAM model, but dissipation is allowed under mean loads (Jostad et al., 2015; Andersen et al., 1994). It uses an effective stress model for the mean load component. However, undrained behaviour during a single cyclic amplitude is assumed. In addition, stress equilibrium and strain compatibility are considered. If large stress redistributions are expected, an iterative calculation procedure is performed. The input parameters for the PDCAM model are the contour plots from undrained cyclic laboratory tests, drained triaxial tests as well as oedometer and permeability test results.

Summarizing, it can be stated that accumulated excess pore pressures around cyclically loaded foundations under a large number of cycles can be calculated with explicit models. However, the existing models are relatively complex. Therefore, in the paper at hand, a new explicit model focusing on practical applicability is presented. In this model, a relatively simple material law for the sand soil is applied and only undrained cyclic DSS tests are required as input. It is hypothesized that even with such a simplified model the capacity degradation of foundation systems can be suitably approximated, which of course has to be proven by comparison with model or field test results. However, at the time being the validation of all the presented methods considering excess pore pressure accumulation is difficult to achieve because there are very few well-documented, high-quality tests in sand under partially drained conditions. Therefore, the execution of high-quality model tests is the next step in the ongoing research.

3. Behaviour of sand in undrained cyclic DSS tests

The method presented here for estimating cyclically accumulated excess pore water pressures uses as input parameters for describing cyclic soil behaviour the results of a series of cyclic undrained simple shear tests. A result of such a test is exemplarily shown in Fig. 2. A soil sample is first consolidated under a given normal stress σ_{v0} (which is identical to the initial effective normal stress σ'_{v0}). Subsequently, a cyclic shear stress with mean value τ_{mean} and amplitude τ_{cyc} is applied (Fig. 2 (a)). Under undrained conditions, this results in excess pore water pressure accumulation with an increasing number of cycles (Fig. 2 (b)).

As an alternative to an undrained test, a drained test can also be performed with dry sand under constant-volume (CV) condition. The constant-volume conditions can be assumed equal to undrained conditions according to ASTM D8296-19 (see also Finn and Vaid, 1977).

Using the initial effective normal stress as a reference value, the stress conditions and also the results of a cyclic DSS test can be presented in dimensionless form. Cyclic stress ratio (*CSR*) and mean stress ratio (*MSR*) characterize the loads. The load type ratio (*LTR*) results from the quotient of the two stress ratios:

$$CSR = \frac{\tau_{cyc}}{\sigma'_{v0}} \tag{2}$$

$$MSR = \frac{\tau_{mean}}{\sigma'_{v0}} \tag{3}$$

$$LTR = \frac{MSR}{CSR} \tag{4}$$

The excess pore pressure Δu is also related to the initial effective normal stress and can be expressed as the normalized excess pore pressure ratio R_u:

$$R_u = \frac{\Delta u}{\sigma'_{v0}} \tag{5}$$

Also R_u exhibits a mean value and a cyclic amplitude (cf. Fig. 2 (b)). The mean value is usually taken as decisive for the accumulative behaviour.

The results of a test series with variable *CSR* and *MSR* values can be displayed graphically in contour plots. Fig. 3 shows such contour plots, from which the R_u-value can be read for a certain number of cycles *N* as a function of *CSR* and *MSR*. Such contour plots thus characterize the soil behaviour under cyclic undrained shearing. It should be noted that in these tests, the mean shear stress (*MSR*) was initially applied in a drained manner and only the cyclic amplitudes were subsequently applied under undrained conditions (CV).

For performing calculations, it is convenient to describe the results contained in the contour plots using analytical equations. Seed et al. (1975), building on studies by De Alba et al. (1975), have proposed a parametrization of the results of cyclic triaxial tests by Lee and Seed (1967). They first proposed an approach for calculating the number of load cycles N_{liq} leading to complete liquefaction (R_u = 1 or, alternatively, vertical double strain amplitude ε_a = 5%):

$$N_{liq} = \left(\frac{CSR}{D_r\, a}\right)^{-\left(\frac{1}{b}\right)} \tag{6}$$

Here D_r is the relative density of the sand and *a* and *b* are regression parameters.

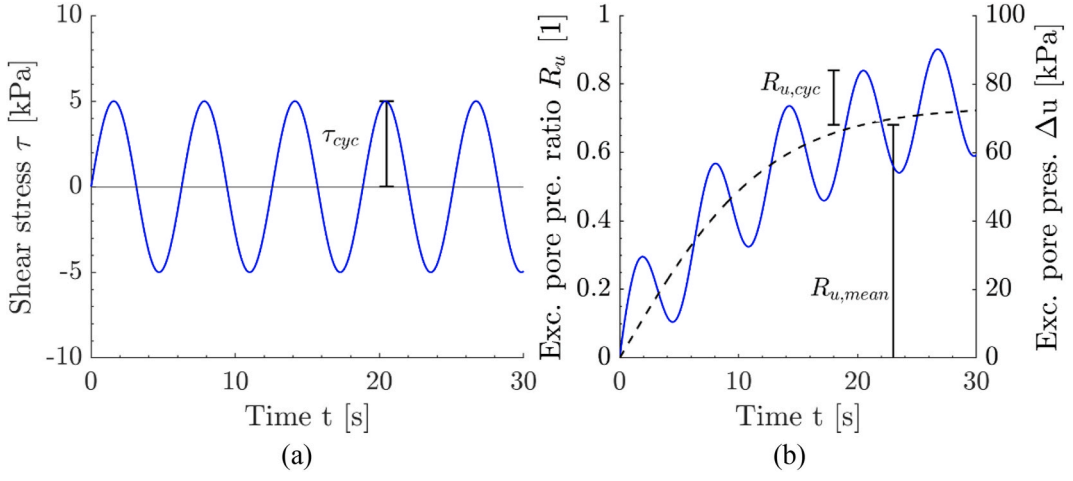

Fig. 2. Shear stress loading condition (a) and resulting excess pore pressure trend (b) of a cyclic undrained DSS test (schematic).

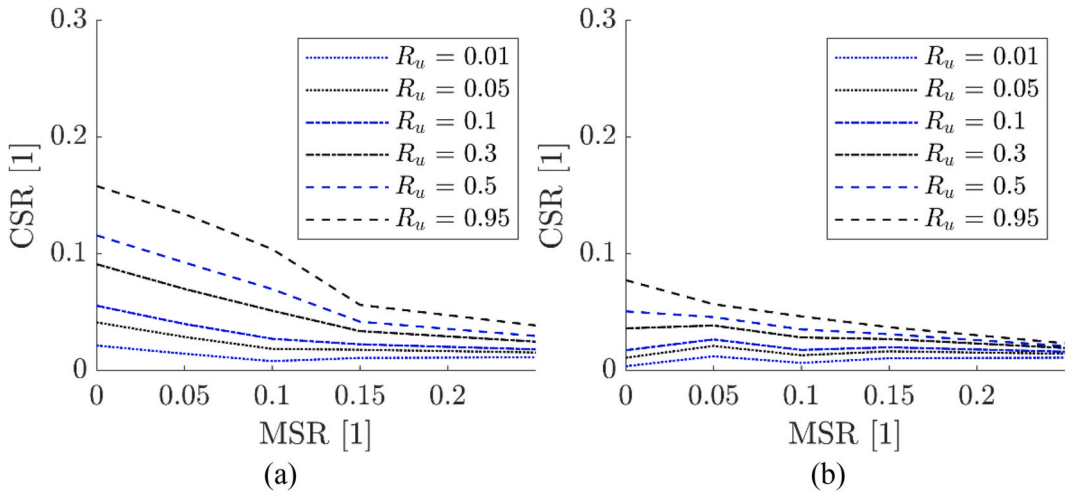

Fig. 3. Excess pore pressure ratio contour plots for N = 10 (a) and N = 1000 (b) from cyclic DSS test performed by the authors for a fine sand with $C_u = 1.80$ and $C_c = 1.02$.

The excess pore water pressure ratio R_u associated with a given number of cycles N is then formulated as a function of N_{liq}:

$$R_u = \frac{1}{2} + \frac{1}{\pi}\, asin\left(2\left(\frac{N}{N_{liq}}\right)^{\frac{1}{\beta}} - 1\right) \tag{7}$$

In this equation, β is another regression parameter. The regression parameters are valid for a predefined *MSR*, i.e. the dependency on *MSR* has to be described by further fitting parameters.

Based on the results of numerous cyclic DSS tests with a poorly graded medium sand, in which CSR- and MSR-values were systematically varied, the authors developed Equation (8) to parameterize the contour plots. More or less by trial and error, a function was sought which on the one hand is practical applicable and gives on the other hand an overall good agreement with the test results.

$$CSR = \tanh\left(a_1 \bullet R_u^{a_2}\right) \bullet \left(\ln(1000) - \ln(N)\right)^2 + \tanh\left(b_1 \bullet R_u^{b_2}\right) \tag{8}$$

This equation is valid for a maximum cycle number of 1000 and contains four regression parameters a_1, a_2, b_1 and b_2, which must be determined as a function of *MSR*. The parameter set determined by regression analyses for a relative density of the sand of $D_r = 0.85$ is presented in Table 2 (section 4.2), as this parameter set was applied also in the numerical simulations presented here. Equation (8) has proven to be well-suited for describing the relationship between *CSR*, *MSR*, *N* and R_u for sands investigated by the authors. Fig. 4 shows contour plots for MSR = 0 and MSR = 0.1 according to Equation (8) in comparison to experimental results.

4. New explicit method for excess pore pressure estimation

4.1. General

The basic idea of the new explicit method is to use a relatively simple numerical simulation model, which could also easily be used in practice. In practical projects, data regarding the behaviour of soil layers are usually limited. Therefore, it is desirable to use only parameters for which broad experience exists and which can easily be correlated with field test data. Of course, results of cyclic DSS tests are required in the method, which at the time being necessitates a comprehensive laboratory test program. However, with more experience regarding the behaviour of sands in cyclic undrained DSS tests, a sufficiently accurate estimation of contour plots might in future be possible based on standard soil parameters and scaling approaches.

In the following, an idealized load due to a storm event is assumed, namely a cyclic load with constant amplitude $F_{cyc} = 0.5\,(F_{max} - F_{min})$ and constant mean value $F_{mean} = 0.5\,(F_{max} + F_{min})$ as well as a given number of cycles N_{equ}. An actual storm event naturally consists of many load cycles with variable amplitude and mean value. However, it is possible and common to convert such a storm event into an event with a constant reference load (usually the extreme load) with an equivalent load cycle number. In addition, in order to take drainage effects into account, the duration of a load cycle T_{cyc} must be defined.

The calculation according to the new method is done in three steps (cf. Fig. 5):

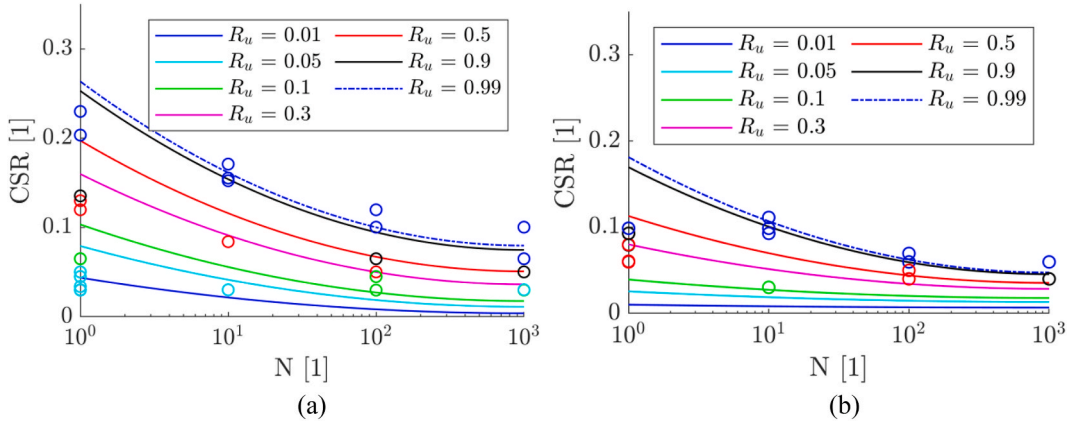

Fig. 4. Excess pore pressure contour plots for MSR = 0.0 (a) and MSR = 0.1 (b) from Equation (8) compared to the results of cyclic DSS tests.

- First, the system behaviour under monotonic drained load is calculated with the numerical model. On the one hand, this results in the capacity (ultimate load) without taking the storm event into account. Secondly, the input values for the evaluation of the contour plots are obtained from the soil stresses under the effect of the loads F_{mean} and F_{max}. From these, the excess pore water pressures are obtained for each soil element of the system assuming undrained conditions, using the results of the cyclic DSS tests.
- Secondly, to take the drainage effects during the storm event into account, a consolidation calculation is performed with the numerical model using the determined excess pore water pressures. This results in a decay curve for each soil element, which describes the reduction of the excess pore water pressure with time. This decay curve is used, taking into account the load cycle duration T_{cyc}, to calculate the reduction of the excess pore water pressure occurring during the storm event by means of an analytical procedure.
- In the third step, the ultimate load of the system is recalculated with the numerical model, taking into account the determined excess pore water pressures and thus the reduction of the effective stresses in the soil. This will quantify the reduction of the ultimate load due to the storm event.

In the following, a reference system is first defined, on which the individual steps of the calculation method are then presented and explained.

4.2. Numerical model of a reference system

In the following, a reference monopile shall be used with a diameter of $D = 9\ m$ and an embedded length of $L = 27\ m$ with a load eccentricity of $e = 40\ m$ (Fig. 6 (a)). The wall thickness is assumed to be constant with $t = 100$ mm. An equivalent number of cycles was set to $Neq = 30$ for all calculations. The sand has a permeability of $k_f = 3.7\ 10^{-4}$ m/s for a relative density of $Dr = 0.85$. The monotonic bearing capacity was derived from a monotonic simulation to $Fult = 37.4$ MN for a deformation criterion of 0.1D (Fig. 6 (b)). The monopile behaviour is investigated under a symmetric one-way load with a maximum load of 13.6 MN ($Fmin = 0$ MN, $Fmax = 13.6$ MN).

The described analysis was carried out in the finite element program ABAQUS. The three-dimensional numerical model of a monopile consists of approximately 30,000 C3D8(P) elements. Based on the symmetry only one half is modelled to reduce the computational effort (Fig. 6 (a)). In preliminary analyses the mesh resolution and the model dimension have been optimized to reach an appropriate balance of computational effort and sufficiently accurate results. The final model has a width of 12-times the diameter and a depth of 1.5-times the pile length. The model is fixed in all degrees of freedom at the bottom, in normal direction at the periphery and in y-direction at the symmetry plane.

The monopile is modelled with a linear-elastic behaviour with a Young's modulus $E = 2.1 \times 10^8\ kN/m^2$, a Poisson's ratio $\nu = 0.27$ and a buoyant steel unit weight $\gamma'_{steel} = 68$ kN/m^3. The load is applied on a reference point which is connected to the monopile with a coupling constraint.

Regarding the behaviour of the soil, an elasto-plastic material law with Mohr-Coulomb failure criterion and stress-dependent stiffness was used. The stress-dependency is considered with a user defined field in ABAQUS. The linear-elastic, ideal-plastic model with a stress-dependent stiffness modulus considers the main key mechanism of the soil response. Especially, the Mohr-Coulomb material law is sufficiently accurate and does only need a small number of (five) input parameters, which all have clear physical meanings. The stress-dependent stiffness modulus, i.e. the oedometric stiffness, is considered with the following equation:

$$E_s = E_{s,ref} \left(\frac{\sigma'_{oct}}{p_{ref}} \right)^{\lambda} \tag{9}$$

Herein, p'_{ref} is the atmospheric reference stress (100 kPa), σ'_{oct} is the current octahedral effective stress in the considered soil element and $E_{s,ref}$ and λ are soil-dependent stiffness parameters. The soil parameters used are shown in Table 1. The initial horizontal earth pressure at rest was calculated according to $k_0 = 1 - \sin(\varphi')$ and the angle of dilatancy with $\psi = \varphi' - 30$ (non-associated flow rule).

Table 2 shows the used input parameters for Equation (8) in order to consider the excess pore pressure accumulation for a reference relative density of $D_r = 0.85$. The values are sorted by the fitted MSR value.

For the contact modelling the elasto-plastic master-slave concept between the monopile and the adjusted soil was used in a way that a connection between the soil and the structure is present as well as their relative displacement is possible. The maximum coefficient of friction in the sand-steel interface is set to $\delta = 2/3\ \varphi'$ and linearly mobilized within an elastic slip value of $du_{el} = 1$ mm.

The calculation is executed in several steps. First, the initial conditions are set, in which the horizontal stress is calculated. Subsequently, the monopile and the contact are activated with a wished-in-place method. Afterwards, the mean lateral and the related moment and eventually the maximum lateral load are applied. For the consolidation analysis, the ABAQUS model is extended in order to enable a coupled pore fluid and stress analysis. Actually, a hydraulical and mechanical coupled analysis is not necessarily required, because also from an uncoupled flow net analysis suitable pore pressure decay curves could be gained. However, here a coupled analysis was conducted, but for the sake of simplicity the soil behaviour was modelled as linear elastic, using the elastic parameters of the Mohr-Coulomb material law. Therefore, the drained model was converted into a simple linear-elastic coupled model by changing the element type to C3D8P. The boundary conditions were adapted for the additional degree of freedom. The weight of the pore fluid is set to $\gamma_{water} = 10$ kN/m^3.

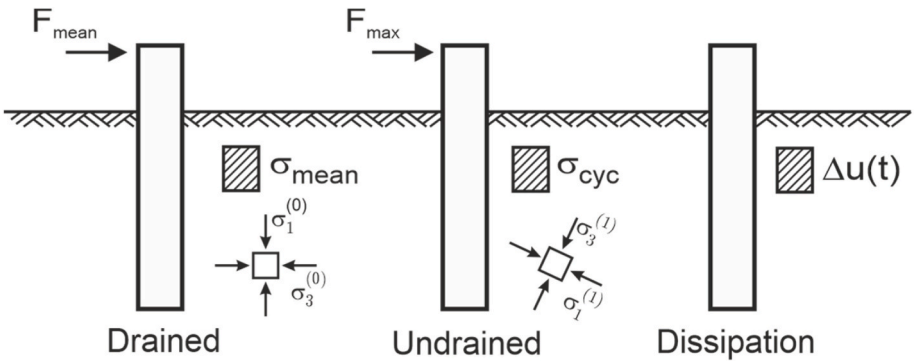

Fig. 5. Steps of Excess Pore Pressure Estimation (EPPE) concept.

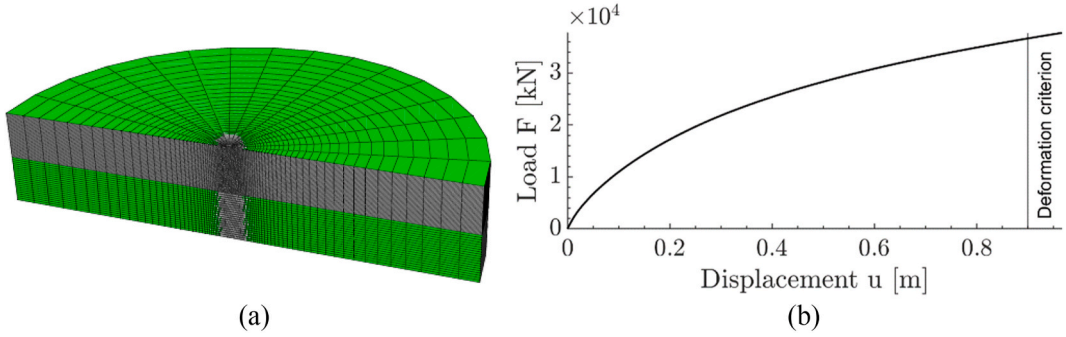

Fig. 6. Overview of numerical reference model (a) and load-displacement curve at mudline (b).

Table 1
Soil properties for numerical calculation.

$E_{s,ref}$	λ	υ	φ′	c′	δ	k_f	ψ	γ′
[MPa]	[1]	[1]	[°]	[kPa]	[°]	[m/s]	[°]	[kN/m³]
67	0.5	0.25	38	0.1	2/3 φ′	$3.7\ 10^{-4}$	8	11

Table 2
Regression parameters for cyclic excess pore pressure ratio contour plot for a relative density of $D_r = 0.85$.

MSR	a_1	a_2	b_1	b_2
[1]	[1]	[1]	[1]	[1]
0.00	0.0205	0.3328	0.0804	0.6601
0.05	0.0201	0.7823	0.0580	0.3353
0.10	0.0150	0.800	0.0476	0.4265
0.15	0.0050	0.900	0.0378	0.2744
0.35	0.0041	0.900	0.0237	0.1624

4.3. Calculation steps and results

4.3.1. Load application and derivation of excess pore pressures

To determine the cyclic stresses relevant for excess pore water pressure development, the stress states in the elements are evaluated under the load F_{mean} and under the load F_{max}. The effective octahedral stress (or mean normal stress) σ'_{oct} and the equivalent octahedral shear stress τ_{oct} are determined as representative values for the normal stress and the shear stress of a three-dimensional stress state:

$$\sigma'_{oct} = \frac{\sigma'_1 + \sigma'_2 + \sigma'_3}{3} \tag{10}$$

$$\tau_{oct} = \sqrt{\frac{2}{9}} \sqrt{\frac{1}{2}\left[\left(\sigma'_{xx} - \sigma'_{yy}\right)^2 + \left(\sigma'_{xx} - \sigma'_{yy}\right)^2 + \left(\sigma'_{xx} - \sigma'_{yy}\right)^2\right] + 6\left[\tau_{xy}^2 + \tau_{yz}^2 + \tau_{xz}^2\right]} \tag{11}$$

Mean stress ratio and cyclic stress ratio are calculated from these quantities with the following equations:

$$MSR_{FE} = \frac{\tau_{oct,Fmean} - \tau_{oct,Fmin}}{\sigma'_{oct,Fmean}} \tag{12}$$

$$CSR_{FE} = \frac{\tau_{oct,Fmax} - \tau_{oct,Fmean}}{\sigma'_{oct,Fmean}} \tag{13}$$

In principle, both the mean and the maximum load could be applied assuming undrained conditions. The mean load, however, is considered here to be a long-term load and thus a drained load. For the cyclic load amplitude, on the other hand, it would have to be considered undrained in any case. For the model version presented here, however, a drained load application is assumed, which means that a hydraulic-mechanical coupled calculation on the numerical model can be dispensed with. Comparative calculations have shown that this assumption for the system investigated here has only small effect on the resulting excess pore pressure fields and capacity reductions (cf. Saathoff, 2023).

Another assumption is made by considering the effective octahedral stress under the mean load as a reference value in equations (12) and (13). In fact, σ'_{oct} is variable over the load increase from F_{min} to F_{max}. However, considering the value at the mean load F_{mean} is a suitable and convenient assumption.

Fig. 7 shows the stress magnitudes determined for the reference system and the resulting distribution of *CSR* and *MSR* values in the plane of symmetry as well as at the soil surface. The horizontal load acts from left to right. The needed stresses to derive *CSR* and *MSR* are depicted in Figure (a)–(c). Fig. 7 (d) clearly shows that large relative shear stresses occur in the near-surface region in front of the monopile in terms of the *CSR* value. The *CSR* values decrease with increasing distance from the monopile and with increasing depth. The maximum *CSR* value in Fig. 7 (d) was set to 0.35 for better readability since for this value a liquefaction is expected after only one cycle.

Also, the *MSR* values are maximal in the passive near-surface region in front of the monopile (Fig. 7 (e)). In this region with large *CSR* values, the *LTR* value is close to 1 (i.e. $MSR \approx CSR$), which is depicted in Fig. 7 (f).

Before the excess pore water pressure ratio can be read from the contour plots, the *CSR* and *MSR* values of the numerical model (CSR_{FE}, MSR_{FE}) must be converted to the specific stress state in the DSS test (CSR_{DSS}, MSR_{DSS}). The initial vertical stress σ'_{v0} in the DSS test is accompanied by a radial or horizontal stress of $\sigma'_{h0} = k_0\ \sigma'_{v0}$. In this, k_0 is the coefficient of earth pressure at rest. Accordingly, the following equation applies:

$$\sigma'_{oct,0} = \frac{1 + 2k_0}{3}\ \sigma'_{v0} \tag{14}$$

Thus, the *CSR* and *MSR* values derived from the numerical model are to be converted as follows:

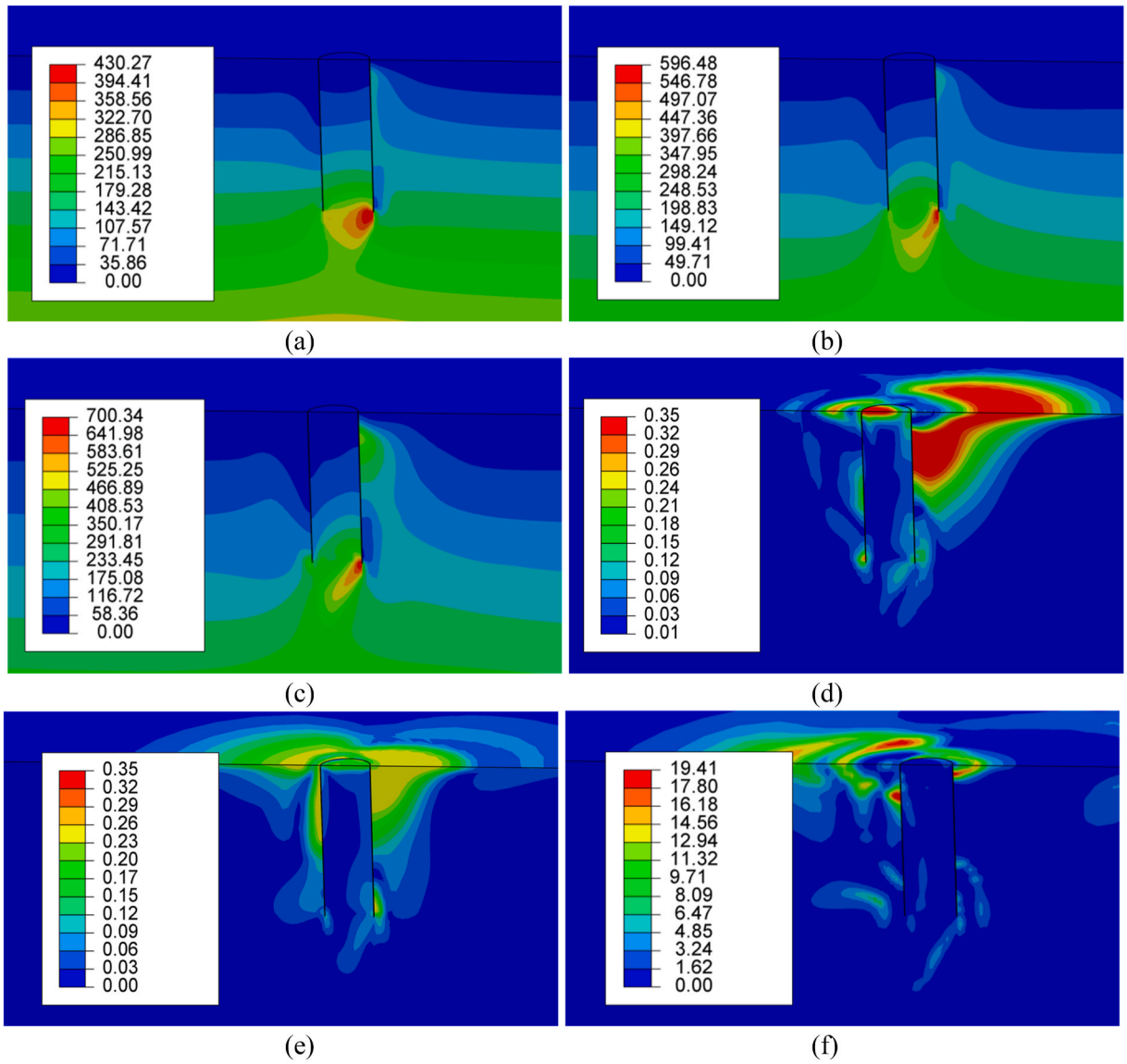

Fig. 7. Stress quantities calculated for the reference system in [kPa] or [1]: a) $\sigma'_{oct,Fmean}$, b) $\tau_{oct,Fmean}$, c) $\tau_{oct,Fmax}$, d) CSR_{FE}, e) MSR_{FE}, f) LTR.

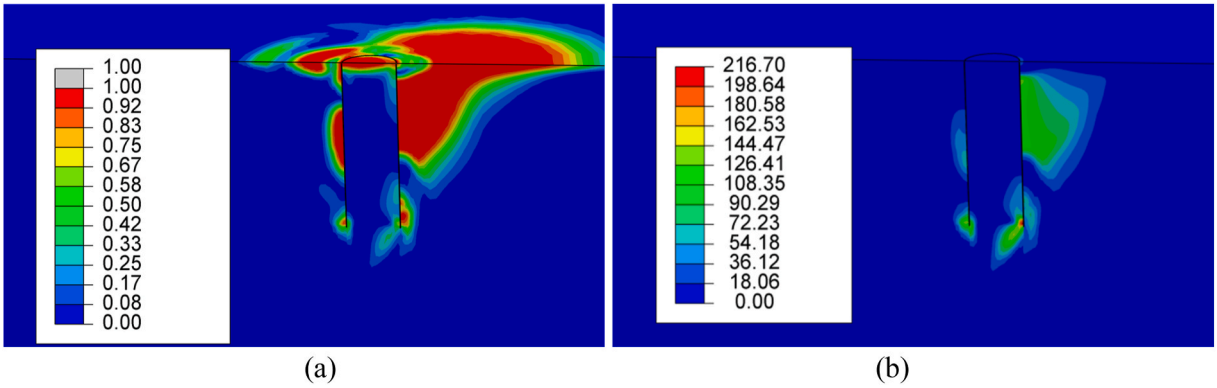

Fig. 8. Excess pore pressure ratio R_u (a) and excess pore pressure Δu (b) prior to dissipation for $N = 1$.

$$MSR_{DSS} = MSR_{FE} \frac{3}{1 + 2 \bullet k_0} \quad (15)$$

$$CSR_{DSS} = CSR_{FE} \frac{3}{1 + 2 \bullet k_0} \quad (16)$$

For the reference system discussed here as an example, k_0 was calculated from the angle of internal friction using the equation $k_0 = 1 - sin\,\varphi'$.

The excess pore water pressure ratios derived with these values from the contour plots for the number of load cycles $N = 1$ are shown in Fig. 8. It can be seen that the largest excess pore water pressures occur where the largest *CSR* values are also present (compare with Fig. 7 (d)). The field looks very similar for different number of cycles, because of large *CSR* values which result in theoretical liquefaction directly after one cycle. For an increased number of cycles, the field with maximum damage will slightly increase in its spatial extension.

4.3.2. Consideration of drainage effects

Considering completely undrained conditions while neglecting drainage effects during a storm event would be unduly conservative for sandy soils. Therefore, the drainage effect must be taken into account. This is done in the new calculation method by means of a consolidation calculation using the excess pore water pressure distribution due to undrained loading with $N = 1$. A flow net calculation is performed with the same numerical model as for the stress calculations. The decisive parameter in this calculation is the hydraulic conductivity k_f of the individual soil layers. The results are specific decay curves for each soil element of the numerical model, which describe the decrease of the excess pore water pressure with the consolidation time. If the values are related to the initial excess pore pressure, location-specific related decay curves are obtained. Fig. 9 shows the calculated decay curves for selected points of the reference system. The points are 3 m in front of the pile and at four different depths below mudline (A: 2 m, B: 5 m, C: 27 m and D: 40 m). Under the pile (point D) there is almost no excess pore pressure. At the top of the model there is a fast dissipation due to the hydraulic boundary condition, whereas for a depth of 5 m (point B), the largest initial excess pore pressure from the four curves is derived. Interestingly, the decay in all curves near the pile (points A, B and C) is quite similar when normalized by their initial value.

The excess pore water pressure taking dissipation into account is calculated separately for each soil element of the system by means of the element-specific decay curves, where the wave period, i.e. the time T_{cyc} between two successive load maxima, is decisive here. For each element, the increase in excess pore water pressure ratio is derived from the contour plots for the governing *CSR* and *MSR* with load cycle number at undrained conditions (Δu generation). The normalized decay curve is then used to determine the pore pressure decrease from cycle to cycle, accounting for the drainage time T_{cyc} (Δu dissipation). Because a constant mean stress is assumed in this process, the excess pore pressure ratio and the absolute excess pore pressure are interchangeable.

For the latter step, an assumption regarding the superposition of the load cycles has to be made. One possibility is to shift the $\Delta u(N)$ curve horizontally to the current (Δu, t_i) point (Fig. 10 (a)). This procedure is based on the idea that the residual excess pore pressure after dissipation is back-calculated to a new number of cycles on the very curve. In doing that, with each cycle an additional excess pore pressure is generated, i.e. with this method a state in which dissipation is greater than dissipation cannot be reached. This is surely conservative.

Another possibility to superpose the load cycles is to shift the $\Delta u(N)$ curve to the current (Δu, t_i) point vertically (Fig. 10 (b)). This procedure seems more realistic and was first described by Hyodo et al. (1988). The predicted build-up trend for the excess pore pressure compares well with partially drained triaxial tests reported in the literature (e.g. Ni et al., 2012), where after several cycles a peak value and afterwards a decrease of excess pore pressure was observed. Fig. 11 compares the two alternatives for an example. With the „horizontal shifting" procedure (blue curve), a considerably higher maximum excess pore pressure is determined than with the „vertical shifting" procedure (black curve). Although the latter method is deemed more realistic than the former, both procedures were applied here for the reference system in order to compare the results.

The excess pore water pressure field after taking dissipation into account (using the "horizontal shifting" procedure) is shown for the investigated reference system in Fig. 12. Fig. 12 (a) shows the relative and Fig. 12 (b) the absolute excess pore pressure, where both are correlated with the octahedral stress at global mean load in the three-dimensional stress state (cf. Equations (5) and (13)). It can be seen that the short drainage paths near the surface lead to a significant reduction of the values determined for the undrained case (see Fig. 8). The maximum relative and also the absolute excess pore water pressures occur in the middle passive area in front of the monopile (here at depths between about 5 and 8 m). Below the rotation point of the monopile, where bedding resistance is mobilized on the other side of the pile, the excess pore water pressures remain small.

Fig. 13 (a) shows the final excess pore pressure field for the "vertical shifting" method. The dissipation effect, which leads to smaller final excess pore pressure ratios compared to Fig. 12 (a), can clearly be seen. To use the "vertical shifting" method more conservatively, Fig. 13 (b) shows the final field using "vertical shifting" but taking the maximum value in the trend over time (cf. Fig. 11). In this way, it neglects the state where the excess pore pressure decreases to zero for an increasing number of cycles. When comparing Figs. 12 (a) and Fig. 13 (b) similar excess pore pressure ratio fields can be seen, because the conservative approach ("horizontal shifting" method) derives similar maximum

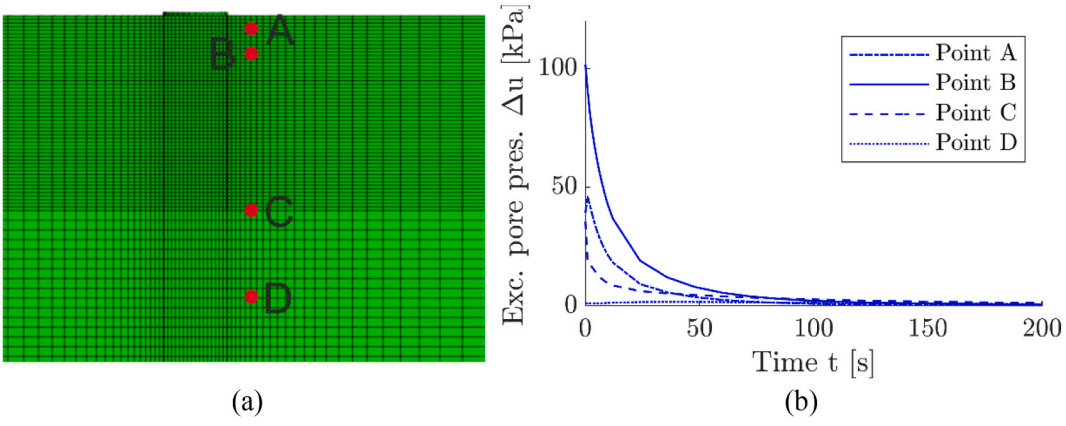

Fig. 9. Locations of investigated points (a) and exemplary excess pore water pressure decay curves for the monopile system (b).

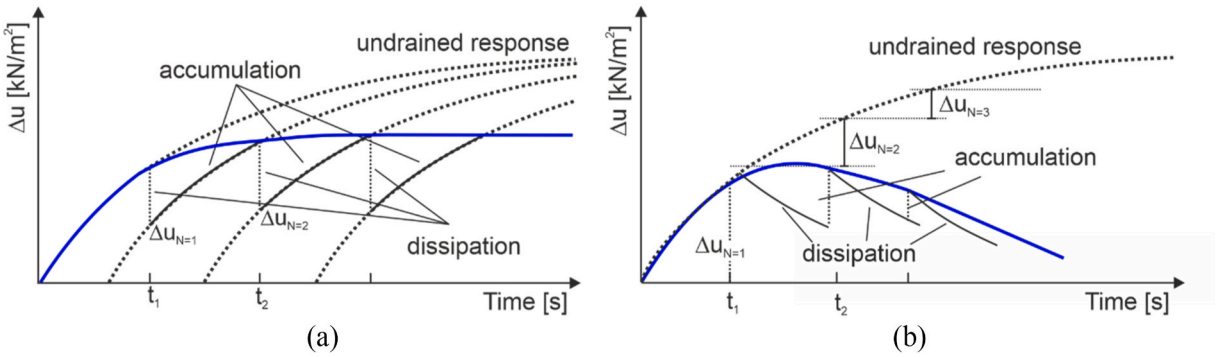

Fig. 10. Methods for analytical dissipation superposition: (a) horizontal shifting and (b) vertical shifting of the $\Delta u(N)$ curve.

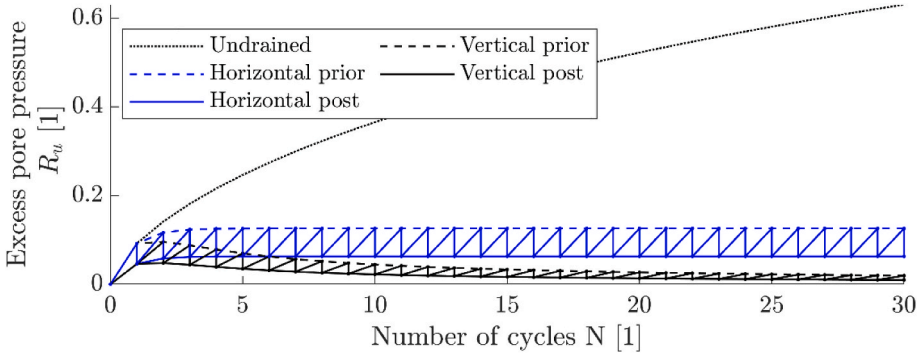

Fig. 11. Exemplary comparison of the „horizontal shifting" and „vertical shifting" procedures for the superposition of load cycles in dissipation calculation.

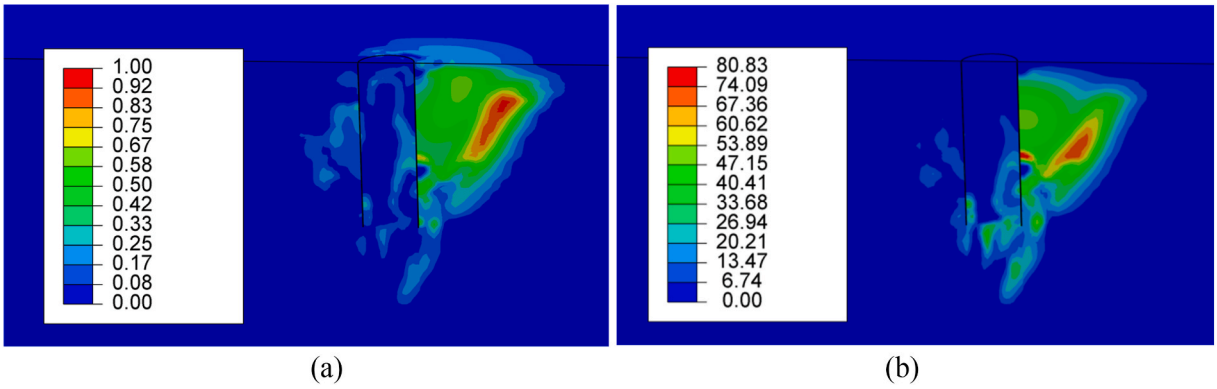

Fig. 12. Final excess pore pressure ratio field R_u (a) and absolute excess pore pressure Δu (b), calculated with the „horizontal shifting" dissipation procedure.

excess pore pressures compared to the maximum in the "vertical shifting".

4.3.3. Calculation of reduced capacity

In the final step of the new calculation model, the determined excess pore water pressures from Fig. 12 (a) or Fig. 13 are taken into account in the bearing capacity calculation. The excess pore water pressures reduce the effective stresses in the soil and thus also the bearing capacity of the foundation. If only the bearing capacity is to be determined, the corresponding effect can be taken into account for non-cohesive soils in a simplified way by reducing the internal friction angle for the individual soil elements according to the following equation:

$$\varphi'_{red} = \text{atan}\left((1 - R_u) \bullet tan\ \varphi'\right) \tag{18}$$

Accordingly, in the last step of the calculation, the calculation of the monotonic load-carrying capacity is repeated in the numerical model, taking into account the element-specific reduced friction angles. The load-deformation curves determined for the three dissipation approaches shown are compared in Fig. 14 with the drained load-deformation curve (cf. Fig. 6) for the reference system. If the ultimate load of the monopile is defined as the load corresponding to a horizontal deformation at the level of the soil surface of 10% of the diameter, the load capacity reduction for the example is 50% when using the "horizontal shifting" procedure and 6% when using the "vertical shifting" procedure. Interestingly, applying the maximum pore water pressures over the storm event calculated with the vertical shifting approach ("vertical shifting (max)"), almost the same capacity reduction as for "horizontal shifting" is obtained.

5. Discussion

With the presented new calculation method, expected excess pore

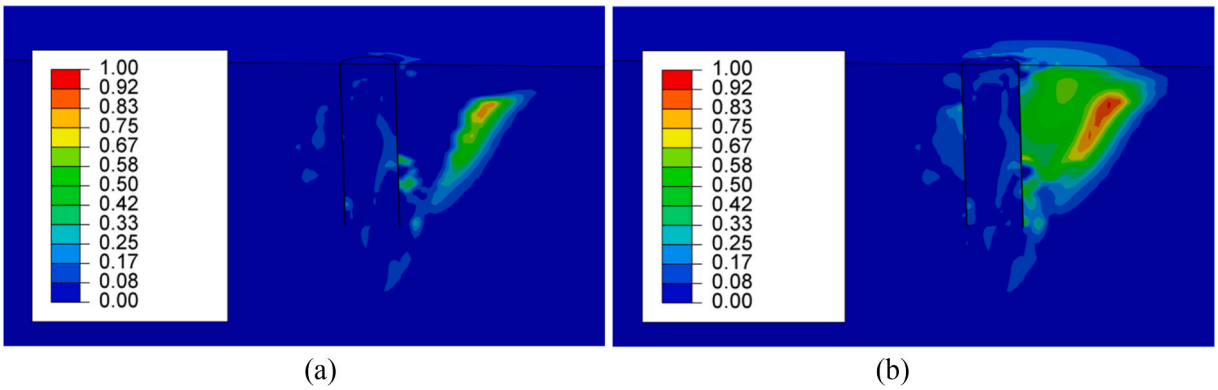

Fig. 13. Final excess pore pressure ratio field R_u for "vertical shifting" (a) and "vertical shifting" (maximum value) (b) after 30 cycles.

water pressures at a foundation system due to an idealized storm load can be quantified and thus the reduction of the bearing capacity can be predicted. Simplifications and idealizations are made at various points in the method to maintain the desired simplicity of application. The acceptability of simplifications can ultimately only be judged by comparing the model results with experimental results. However, the main simplifications in the model will be briefly discussed below.

- The stress boundary conditions were determined in the model presented here by applying not only the mean load but also the cyclic load amplitude assuming drained soil behaviour. This is based on the assumption that drained and undrained loading result in at least similar cyclic stress conditions. A comparative calculation in which the cyclic load amplitude was applied undrained, taking into account hydraulic-mechanical coupled soil behaviour, resulted in a cyclic bearing capacity of the monopile that was about 8% larger. At least for the system considered here, the assumption made is conservative and leads to relatively minor deviations.
- For the normalization of the cyclic stress quantities, the octahedral stress in the elements under the global mean load was used. This is also an assumption because the octahedral stresses change over the load application. Comparison calculations showed that the cyclic bearing capacity of the monopile was about 17% smaller if the octahedral stress under minimum load was used, and about 4% larger if the octahedral stress under maximum load was applied.
- The greatest influence on the bearing capacity results from the assumption made regarding the determination of the excess pore water pressure dissipation in the individual elements. The "horizontal shifting" approach leads to a load-bearing capacity reduction of about 50% for the monopile system considered as an example. However, this approach is clearly very conservative. Using the "vertical shifting" approach results in significantly lower excess pore water pressures at the end of the storm, i.e. after 30 cycles, and a reduction in bearing capacity of only about 6%. However, if the maximum excess pore water pressures occurring during the storm event are taken as the decisive values, the reduction in load-bearing capacity is almost as large as with the "horizontal shifting" approach.

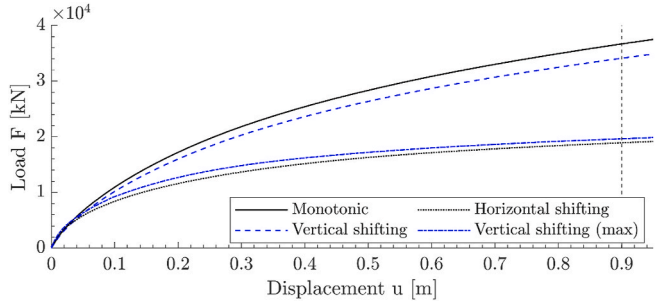

Fig. 14. Load-displacement curve for different maximum lateral loads for symmetric one-way loading for the reference system and EPPE approach with consideration of reduced stiffness.

The admissibility and appropriateness of different model assumptions can only be assessed by comparing calculation and test results. Currently, an extensive validation of the proposed approach is not fully possible. The tests on monopiles under partially drained conditions performed for instance by Taşan (2011) and Kluge (2007) could not be back-calculated due to large acting loads in the medium-scale tests and hence severe liquefaction (Saathoff, 2023). Field tests like the Ekofisk tank are not well documented and can only partially be used for a validation (Clausen et al., 1975). This is mainly because the sensors did not measure during the storm. Additionally, extensive data regarding the cyclic soil response of the used sand is often missing.

A rough classification of the calculation results is possible by comparing them with the results of calculation methods commonly used in practice. The p-y method is usually used for the design of monopiles. The API guideline (API, 2014) contains an approach for determining depth-dependent p-y curves in sandy soils. A distinction is made here between curves for static (monotonic) and cyclic loads. These curves were derived from load test results for instance by Reese et al. (1974), whereby cyclic loads were applied with a maximum of approx. 100 cycles. In practice, it is assumed based on experience that the reduction in load-bearing capacity as a result of the design storm (for which the equivalent number of load cycles is usually significantly less than 100) is sufficiently reliably recorded by applying the cyclic p-y curves.

Investigations have shown that an adaptation of the p-y curves according to API (2014) is necessary for the – due to their large diameter – very stiff monopiles in order to realistically describe the load-bearing behaviour (see e.g. Thieken et al., 2015). Sørensen (2012) has proposed an approach in which only the stiffness parameter of the p-y method according to API (2014) is modified, so that the approach of the API method to take cyclic loads into account remains applicable.

Fig. 15 compares the results of the explicit numerical method presented here with the results of calculations using the p-y method according to Sørensen (2012). To simplify the comparison of the effect of cyclic loading, the friction angle for the calculation with the p-y method was reduced to 35° in order to obtain a similar monotonic load-bearing capacity as determined in the FE model. It can be seen that the cyclic p-y approach results in a reduction of a similar order of magnitude as when assuming the unfavourable dissipation approaches in the application of the numerical method. Although this does not represent a validation of the calculation approach, it proves that plausible results are obtained, at least with regard to the order of magnitude. However, it remains to be clarified whether the unfavourable dissipation approaches and thus ultimately also the cyclic p-y approach are not too conservative.

The presented comparison shows that the EPPE approach yields

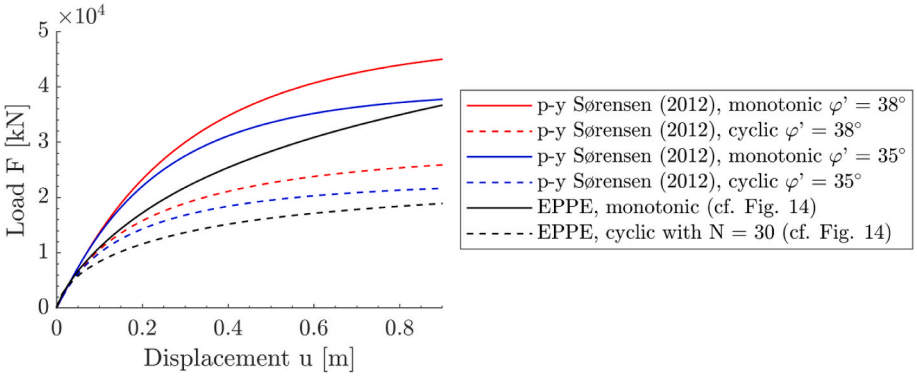

Fig. 15. Comparison of the results from the EPPE approach and results from the p-y approach proposed by Sørensen (2012).

plausible results. However, it must be noted that the new model proposed here yet provides only a conceptual framework to deal with capacity reductions and that a validation of the model by comparison with experimental tests is pending.

6. Conclusions

This paper addresses the problem of bearing capacity reduction of foundation structures in sandy soils due to pore water pressure accumulation by cyclic loads. A new explicit computational model aimed at simple practical application is presented, which requires comparatively simple numerical simulation calculations and as input the results of cyclic undrained direct simple shear tests. The dissipation of excess pore water pressures to be expected in sandy soils in the course of a storm event is estimated by means of an analytical procedure using decay curves determined on the numerical model of the foundation system.

The model application is demonstrated and explained on an exemplarily considered reference system of a monopile in homogeneous sandy soil. The influence of different model assumptions is discussed. It is found that the assumptions made regarding representative stress variables on the system are of comparatively little importance compared to the procedure for estimating excess pore water pressure dissipation.

The computational model presented first provides a conceptual framework for estimating bearing capacity reductions due to pore water pressure accumulation. For the system considered, it yields plausible results and thus appears to be a promising tool for quantifying expected excess pore water pressures and bearing capacity reductions of foundation structures under cyclic loads. However, the appropriateness and reasonableness of various assumptions and idealizations must ultimately be evaluated by comparing the model results with experimental results. Such experiments are planned in an ongoing research project (Collaborative Research Centre 1463, see Schuster et al., 2021). The model is modular, which means that model assumptions can be easily adapted (possibly at the cost of higher computational effort) if this proves necessary.

CRediT authorship contribution statement

Jann-Eike Saathoff: Conceptualization, Data curation, Investigation, Visualization, Writing – original draft, Writing – review & editing. **Martin Achmus:** Conceptualization, Funding acquisition, Supervision, Visualization, Writing – original draft, Writing – review & editing.

Declaration of competing interest

The authors declare that they have no known competing financial interests or personal relationships that could have appeared to influence the work reported in this paper.

Data availability

Data will be made available on request.

Acknowledgement

The investigations reported were funded by the Deutsche Forschungsgemeinschaft (DFG, German Research Foundation) - SFB1463 – 434502799. The support is gratefully acknowledged.

References

Achmus, M., Kuo, Y.S., Abdel-Rahman, K., 2009. Behavior of monopile foundations under cyclic lateral load. Comput. Geotech. 36, 725–735. https://doi.org/10.1016/j.compgeo.2008.12.003.

Achmus, M., Saathoff, J.E., Thieken, K., 2018. Numerical method for evaluation of excess pore pressure build-up at cyclically loaded offshore foundations. Numerical Methods in Geotechnical Engineering IX, 1461–1468. https://doi.org/10.1201/9781351003629-184.

Andersen, K.H., 1976. Behaviour of clay subjected to undrained cyclic loading. In: Behaviour of Offshore Structures. Proceedings of the First International Conference.

Andersen, K.H., Hansteen, O.E., Høeg, K., Prevost, J.H., 1978. Soil Deformations Due to Cyclic Loads on Offshore Structures. Norwegian Geotechnical Institute Publication.

Andersen, K.H., Allard, M.A., Hermstad, J., 1994. Centrifuge model tests of a gravity platform on very dense sand; II: interpretation. others (Elsevier). In: Chryssostomidis, C. (Ed.), Proceedings of the 7th International Conference on the Behaviour of Offshore Structures - BOSS'94, pp. 255–282.

API, 2014. Recommended Practice 2GEO-Geotechnical and Foundation Design Considerations. American Petroleum Institute. Version October 2014.

ASTM D8296-19, 2019. Standard test method for consolidated undrained cyclic direct simple shear test under constant volume with load control or displacement control. https://www.astm.org/d8296-19.html.

Bjerrum, L., 1973. Geotechnical problems involved in foundations of structures in the North Sea. Geotechnique 23, 319–358. https://doi.org/10.1680/geot.1973.23.3.319.

Clausen, C.J.F., Dibiagio, E.J.F., Duncan, J.M., Andersen, K.H., 1975. Observed behaviour of the Ekofisk oil storage tank foundation. In: Proceedings of the Offshore Technology Conference, pp. 399–431. https://doi.org/10.4043/2373-MS. Houston, Texas.

Cuéllar, P., 2011. Pile foundations for offshore wind turbines: numerical and experimental investigations on the behaviour under short-term and long-term cyclic loading. PhD thesis. Technische Universität Berlin. https://doi.org/10.14279/depositonce-2760.

Dafalias, Y.F., 1986. Bounding surface plasticity. I: mathematical foundation and hypoplasticity. J. Eng. Mech. 112 (9), 966–987. https://doi.org/10.1061/(ASCE)0733-9399(1986)112:9(966).

Dafalias, Y.F., Manzari, M.T., 2004. Simple plasticity sand model accounting for fabric change effects. J. Eng. Mech. 130 (6), 622–634. https://doi.org/10.1061/(ASCE)0733-9399(2004)130:6(622).

Dafalias, Y.F., Popov, E.P., 1975. A model of nonlinearly hardening materials for complex loading. Acta Mech. 21, 173–192. https://doi.org/10.1007/BF01181053.

De Alba, P., Chan, C.K., Seed, H., 1975. Determination of Soil Liquefaction Characteristics by Large-Scale Laboratory Tests.

DNV-RP-C212, 2019. Offshore Soil Mechanics and Geotechnical Engineering. Standard. Det Norske Veritas.

Dührkop, J., 2009. Zum Einfluss von Aufweitungen und zyklischen Lasten auf das Verformungsverhalten lateral beanspruchter Pfähle in Sand, PhD Thesis, Institut für Geotechnik und Baubetrieb, vol. 20. Technische Universität Hamburg-Harburg, 978-3-936310-21-4, (in German).

Finn, W.D.L., Vaid, Y.P., 1977. Liquefaction potential from drained constant volume cyclic simple shear tests. In: Proceedings of the 6th World Conference on Earthquake Engineering. New Delhi, India.

Grabe, J., Dührkop, J., Mahutka, K.-P., 2004. Monopilegründungen von Offshore-Windenergieanlagen - zur Bildung von Porenwasserüberdrücken aus zyklischer Belastung. Bauingenieur 79, 418–423.

Grabe, J., Mahutka, K.-P., Dührkop, J., 2005. Monopilegründungen von Offshore-windenergieanlagen - Zum Ansatz der Bettung. Bautechnik 82 (1), 1–10. https://doi.org/10.1002/bate.200590020.

Hyodo, M., Yashuhara, K., Murata, H., 1988. Earthquake induced settlements in clays. In: Proceedings of the Ninth World Conference on Earthquake Engineering. URL: https://www.iitk.ac.in/nicee/wcee/article/9_vol3_89.pdf.

Jostad, H.P., Andresen, L., 2009. A FE procedure for calculation of displacements and capacity of foundations subjected to cyclic loading. In: Proceedings of the 1st International Symposium on Computational Geomechanics – GOMGEO I.

Jostad, H.P., Andersen, K.H., Tjelta, T.I., 1997. Analyses of Skirted Foundations and Anchors in Sand Subjected to Cyclic Loading.

Jostad, H.P., Grimstad, G., Andersen, K.H., Sivasithamparam, N., 2015. A FE procedure for calculation of cyclic behaviour of offshore foundations under partly drained conditions. In: Frontiers in Offshore Geotechnics III.

Jostad, H.P., Dahl, B.M., Page, A., Sivasithamparam, N., Sturm, H., 2020. Evaluation of soil models for improved design of offshore wind turbine foundations in dense sand. Geotechnique 70, 682–699. https://doi.org/10.1680/jgeot.19.TI.034.

Kluge, K., 2007. Soil Liquefaction Around Offshore Pile Foundations - Scale Model Investigations. PhD thesis. Faculty of Architecture, Civil Engineering and Environmental Sciences, University of Braunschweig. https://doi.org/10.24355/dbbs.084-200808280200-5.

Kolymbas, D., 1988. Eine konstitutive Theorie für Böden und andere körnige Stoffe. PhD thesis. Institut für Bodenmechanik und Felsmechanik der Universität Fridericiana.

Lambe, W.T., 1967. Stress path method. J. Soil Mech. Found Div. 93, 309–331. https://doi.org/10.1061/JSFEAQ.0001058.

Lee, K.L., Seed, H.B., 1967. Cyclic stress conditions causing liquefaction of sand. J. Soil Mech. Found Div. 93, 47–70. https://doi.org/10.1061/JSFEAQ.0000945.

Manzari, M.T., Dafalias, Y.F., 1997. A critical state two-surface plasticity model for sands. Geotechnique 47 (2), 255–272. https://doi.org/10.1680/geot.1997.47.2.255.

Ni, J., Indraratna, B., Geng, X.Y., Carter, J.P., Rujikiatkamjorn, C., 2012. Radial consolidation of soft soil under cyclic loads. Comput. Geotech. 50, 1–5. https://doi.org/10.1016/j.compgeo.2012.11.011.

Niemunis, A., Herle, I., 1998. Hypoplastic model for cohesionless soils with elastic strain range. Mech. Cohesive-Frict. Mater. 2 (4), 279–299. https://doi.org/10.1002/(SICI)1099-1484(199710)2:4<279::AID-CFM29>3.0.CO;2-8.

Niemunis, A., Wichtmann, T., Triantafyllidis, T., 2005. A high-cycle accumulation model for sand. Comput. Geotech. 32, 245–263. https://doi.org/10.1016/j.compgeo.2005.03.002.

Rahman, M.S., Booker, J.R., Seed, H.B., 1977. Pore pressure development under offshore gravity structures. J. Geotech. Eng. Div. 103, 1419–1436. https://doi.org/10.1061/AJGEB6.0000537.

Reese, L.C., Cox, W.R., Koop, F.D., 1974. Analysis of laterally loaded piles in sand. In: Proc. Of Offshore Technology Conf.. No. OTC 2080.

Saathoff, J.E., 2023. Modelling of Excess Pore Pressure Accumulation in Sand Around Cyclically Loaded Foundations. Ph.D. thesis. Institut für Geotechnik, Leibniz Universität Hannover.

Saathoff, J.E., Achmus, M., 2020. Practical approach for the evaluation of cyclically induced excess pore pressure around offshore foundations in sand. In: Proceedings of the 4th International Symposium on Frontiers in Offshore Geotechnics.

Schuster, D., Hente, C., Hübler, C., Rolfes, R., 2021. Integrierte Entwurfs- und Betriebsmethodik für Offshore-Megastrukturen. Bautechnik 98, 563–570. https://doi.org/10.1002/bate.202100044.

Seed, H.B., Martin, P.P., Lysmer, J., 1975. The Generation and Dissipation of Pore Water Pressures during Soil Liquefaction. College of Engineering, University of California.

Sørensen, S.P.H., 2012. Soil-structure interaction for non-slender large-diameter offshore monopiles. PhD Thesis. Aalborg University Denmark, Department of Civil Engineering.

Taiebat, H.A., 1999. Three Dimensional Liquefaction Analysis of Offshore Foundations. Ph.D. thesis. Department of Civil Engineering, University of Sydney.

Taşan, H.E., 2011. Zur Dimensionierung der Monopile-Gründungen von Offshore-Windenergieanlagen. PhD thesis. Technische Universität Berlin (in German).

Taşan, H.E., Rackwitz, F., Savidis, S., 2010. Porenwasserdruckakkumulation bei zyklisch horizontal belasteten Monopiles mit großen Durchmessern. Bautechnik 87 (8), 449–461. https://doi.org/10.1002/bate.201010032 (in German).

Thieken, K., Achmus, M., Lemke, K., Terceros, M., 2015. Evaluation of p-y approaches for large diameter monopiles in sand. Int. J. Offshore Polar Eng. 25 (2), 134–144. June 2015.

Von Wolffersdorff, P.A., 1996. A hypoplastic relation for granular materials with a predefined limit state surface. Mech. Cohesive-Frict. Mater. 1 (3), 251–271. https://doi.org/10.1002/(SICI)1099-1484(199607)1:3<251::AID-CFM13>3.0.CO;2-3.

Wichtmann, D., 2005. Explicit Accumulation Model for Non-cohesive Soils under Cyclic Loading. Ph.D. thesis. Fakultät für Bauingenieurwesen, Ruhr-Universität Bochum.

Wichtmann, T., Rojas, B., Niemunis, A., Triantafyllidis, T., 2011. Prediction of drained and undrained cyclic behaviour of a fine sand using a high-cycle accumulation model. In: Proceedings of the 5th International Conference on Earthquake Geotechnical Engineering.

Wood, D.M., 1990. Soil Behaviour and Critical State Soil Mechanics. Cambridge University Press.

Zachert, H., Wichtmann, T., 2020. Approaches for the Design of Foundations for Offshore Wind Turbines. Springer. https://doi.org/10.1007/978-3-030-28516-6_7.